



Investigation of the demetallation of 10-aryl substituted synthetic chlorins under acidic conditions

Anna I. Arkhynchuk, Ruisheng Xiong, K. Eszter Borbas*

Department of Chemistry, Ångström Laboratory, Box 523, Uppsala University, 75120 Uppsala, Sweden

ABSTRACT

The acidic demetallation of a series of sparsely substituted Zn(II) chlorins is reported. The chlorins were functionalized in the 10-position with substituents ranging from strongly electron donating mesityl and *p*-methoxyphenyl to electron-withdrawing *p*-nitrophenyl and pentafluorophenyl groups. The demetallation kinetics were investigated using UV-Visible absorption spectroscopy. Demetallation was carried out by exposing the metallochlorins dissolved in CH₂Cl₂ to an excess of trifluoroacetic acid. Reasonable correlation was found between the Hammett constant of the 10-substituent and the rate constant of the loss of the metal ion. The largest differences were observed between the *p*-methoxyphenyl and *p*-nitrophenyl-substituted Zn(II) chlorins, undergoing loss of Zn(II) with pseudo first order rate constants of 0.0789×10^{-3} and $3.70 \times 10^{-3} \text{ min}^{-1}$, respectively. Taken together, these data establish the dramatic influence even subtle changes can have in altering the electronic properties of chlorins, which in turn impacts metallochlorin function.

1. Introduction

Chlorins are 18 π -electron cyclic tetrapyrroles with a porphyrin-like carbon framework but with one less peripheral double bond compared to porphyrins [1–3]. Discovered in 1817, chlorins remain a topic of interest due to their natural abundance. Chlorophylls *a*, *b*, *d* and *f* are chlorins, and as such are central to supporting life on Earth [3]. Chlorins are extensively used as photosensitizers [4–9] and as imaging agents [10–13], and they are versatile components of light-harvesting polymers in artificial photosynthesis [14–17]. The tetrapyrrolic macrocycle provides a tetradentate square planar metal coordination site that can bind a large variety of metal ions [18,19]. Chelation of a metal ion can impart new functionality to the chlorin. Examples include the catalytic activities of cobalt chlorins for proton reduction to H₂ [20] and for the reduction of O₂ to H₂O₂ [21,22]. Chlorins in Nature are found as their metal (Mg(II)) chelates, the stabilities of which are of profound interest for a number of reasons [3]. Free base and metallochlorins have very different properties, including differences in polarity, spectroscopic properties, redox potentials, macrocycle geometry and reactivity [23–26]. The loss of the central metal ion is typically the first step of the chlorophyll degradation [27]. Extensive studies on naturally-occurring or naturally-derived metallochlorins have revealed dramatic differences in the chelate stabilities. In general, electron-withdrawing substituents tend to decrease the sensitivity of metallochlorins to acidic conditions due to a decrease in the basicity of the nitrogen donors [28–31]. However, the complexity of the macrocycle structures precludes the drawing of general conclusions about the

effects of peripheral substituent on chelate stability, and the quantification of the effect individual substituents exert.

For the reasons listed above, a systematic investigation of chlorin demetallation that goes beyond naturally-occurring magnesium chlorophylls is desirable. Scattered evidence suggests a wide range of reactivities, providing a motivation for this study. For example, Battersby removed Cu(II) from an 2,3,7,8,12,13-hexaalkylchlorin using trifluoroacetic acid (TFA) saturated with H₂S (18 h, r.t., 71% isolated yield) [32], while we observed quantitative demetallation of a Cu(II) 10-aryl chlorin under mild conditions (dilute TFA in CH₂Cl₂, r.t.) within minutes [33]. Comparison of Zn(II) porphyrins and chlorins with identical substitution patterns have shown that the metalloporphyrins are more stable under acidic conditions than the chlorins [34]. The effect of macrocycle saturation was relatively modest, with the porphyrin ligand conferring 1.3 to 1.7-fold increased stability to the chelate compared to the chlorin. However, the effect of the substituents was more dramatic. The introduction of electron-withdrawing 3-, 7- or 13-substituents increases the stabilities of both Mg(II) [35,36] and Zn(II) chlorins [30,31]. The effect of such a substitution can be quite dramatic, e.g. a 3-acetyl in the place of a 3-vinyl group slows down acidic demetallation by up to 20-fold [28].

Here, we investigate the kinetics of the chlorin demetallation in a library of stable, sparsely substituted chlorins. The library consists of Zn(II) chlorins carrying only 10-aryl substituents in addition to 18,18-gem-dimethyl substituents. The purpose of the latter is to lock-in the hydrophorphyrin oxidation level, while the aryl substituents modulate the electronic properties of the macrocycle. The acidic demetallation

* Corresponding author.

E-mail address: eszter.borbas@kemi.uu.se (K.E. Borbas).

<https://doi.org/10.1016/j.jinorgbio.2019.110979>

Received 30 September 2019; Received in revised form 11 December 2019; Accepted 24 December 2019

Available online 03 January 2020

0162-0134/ © 2020 Elsevier Inc. All rights reserved.

kinetics were followed by UV–Vis absorption spectroscopy. The rates of the demetallations were then analyzed in the context of macrocycle electronic structure using a combination of ^1H and ^{13}C NMR spectroscopy and cyclic voltammetry. Taken together, these results represent the first systematic investigation of single substituent effects on metallochlorin stability, and provide an entry point for predicting chelate robustness in future applications.

2. Results and discussion

To investigate the demetallation kinetics and the influence of peripheral substituents, we designed a small library of 10-substituted chlorins (**Scheme 1**). The 10-aryls include substituents with electron-neutral (H, **1a**), electron-withdrawing (I, F, NO_2 , Br, F_5 ; **M-1b,e,f,i,k**), electron-donating (2,4,6-tri-Me, 2,6-di-OMe, 4-OMe, 4- $\text{OCH}_2\text{CO}_2^t\text{Bu}$, **M-1c,g,j,l**), sterically demanding (2,4,6-tri-Me, 2,6-di-OMe, **M-1c,g**) properties, as well as heterocyclic groups (thienyl and furanyl, **M-1d,h**).

The chlorins were prepared following a standard two-step procedure developed by Lindsey (**Scheme 1**) [37–39]. Condensation of 1-bromo-9-formyldipyromethanes (Eastern half) [40] with a tetrahydrodipyrin (Western half) [41] yielded Zn(II) chlorins in isolated yields ranging from 4% to 41%. The corresponding free base chlorins were obtained by treating the Zn(II) chlorins with TFA at room

temperature in CH_2Cl_2 solution. Selected free base chlorins were then metallated to obtain the Pd(II) and Cu(II) analogues [33,42]. **Zn-1a, c** [39,43], **Zn-1d** [14], **Zn-1f** [44], **Zn-1g** [45], **Zn-1h** [14], **Zn-1j** [46], **Zn-1k** [46], **Zn-1l** [33] are known compounds, as are **Pd-1a,l** [33] and **Cu-1a,l** [33,39]. Details of the syntheses and standard characterization data are provided in the Experimental section. The characterization data for the known species were in accordance with reported values and with the proposed structures. Selected NMR-spectroscopic, electrochemical and photophysical characterizations are presented below.

3. UV–Vis absorption spectroscopy

In total, 12 free base chlorins were synthesized. These were used as reference compounds for the demetallation products. Additionally, 12 Zn(II) chelates were prepared, along with 5 each of Cu(II) and Pd(II) complexes. With these 34 compounds in hand, we performed a detailed study of their absorption properties, the results of which are presented in **Table 1**. Typical spectra are shown in **Fig. 1**. The UV–Vis absorption spectra of the free base and the metallochlorins were recorded in CH_2Cl_2 . All chlorins had absorptions typical of this class of compounds consisting of two sets of relatively sharp, high intensity bands. The Soret (B) band was located at ~ 400 nm and the Q bands at ~ 500 nm (Q_x) and ~ 600 nm (Q_y). The position of the latter is very sensitive to the

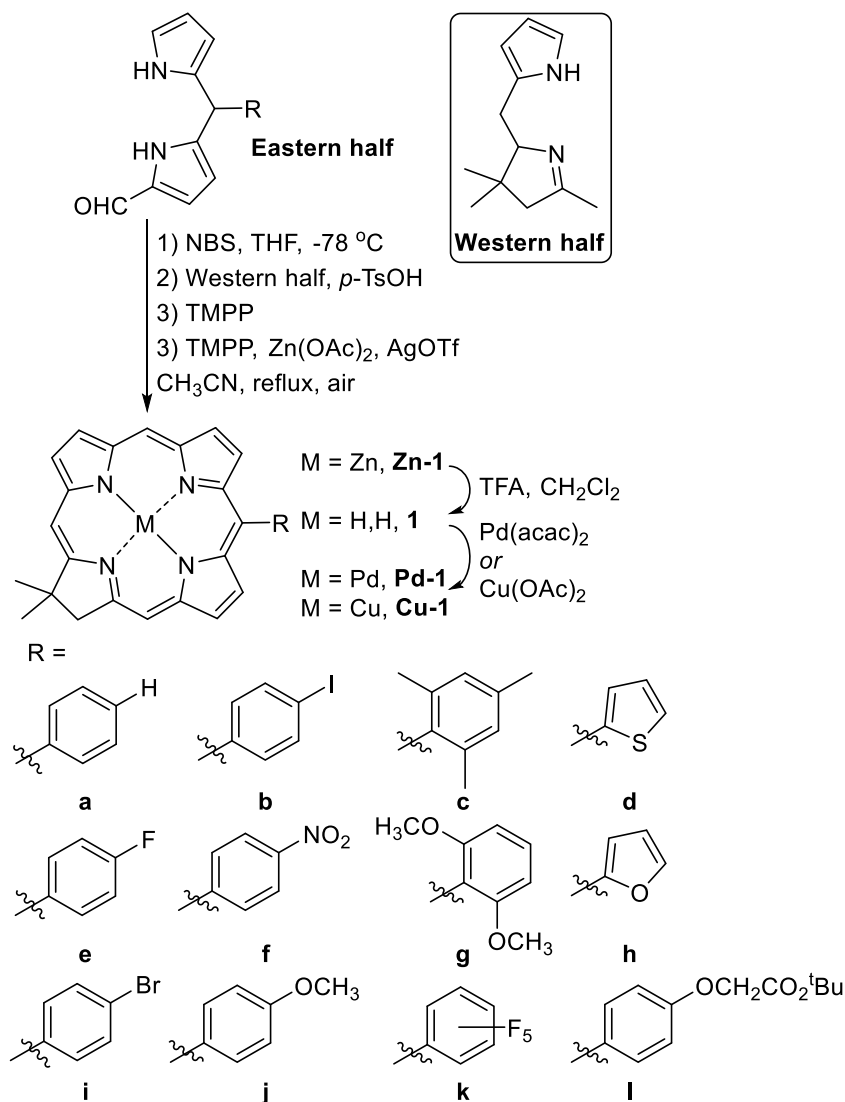


Table 1
Summary of UV–Vis data. Spectra were recorded in CH₂Cl₂, [Chlorin] = $\sim 8 \times 10^{-6}$ M.

	Free base			Zn			Pd			Cu		
	λ_B (nm)	λ_Q (nm)	I_B/I_Q									
a	403	634	4.21	402	604	5.72	393	587	2.66	399	599	5.77
c	404	635	3.74	402	604	5.81						
e	403	634	3.96	402	604	5.85	394	587	2.63	399	599	6.10
i	404	634	4.47	403	604	5.85						
b	404	634	4.46	403	604	5.76						
f	404	636	3.69	402	607	4.51						
j	405	634	4.38	403	604	5.84	395	586	2.68	400	599	5.79
g	404	635	3.96	403	607	5.60	395	588	2.55	400	601	5.76
k	404	635	3.67	404	608	4.73						
d	406	638	4.08	405	609	5.33						
h	406	640	4.32	407	610	4.82						
l	405	634	4.41	403	604	5.60	394	587	2.73	400	600	5.94

macrocycle substitution, albeit the variation induced by alterations of a single meso-substituent is modest. Most of the free base compounds displayed Q_y bands at $\lambda_{\max} = 634\text{--}636$ nm. The only exceptions were the slightly red-shifted absorptions (638 and 640 nm, respectively) of the thienyl- (**1d**) and furylchlorins (**1h**). This may be caused by the small five-membered heterocycle being more co-planar with the macrocycle than the phenyl-based substituents [47].

Metalation hypsochromically shifts the Q_y-band by ~ 30 nm for M = Zn(II), 35–40 nm for M = Cu(II) and 45–50 nm for Pd(II), compared to the analogous free base chlorins. The Soret band is much less sensitive towards the metalation; only for Cu(II) (5 nm) and Pd(II) (10 nm) chelates was a slight hypsochromic shift observed. The ratio of the intensities of the B and Q bands (I_B/I_Q) is also changed upon macrocycle metalation. Introduction of Zn(II) and Cu(II) results in an increased I_B/I_Q ratio from 4:1 in free base compounds to 6:1 in the metallochlorins. Palladation has the opposite effect, decreasing the ratio to 2.5:1. These changes are accompanied by dramatic changes in color observable with the naked eye: free base chlorins are deep green, Zn(II) chelates are bright blue-violet, Pd(II) chelates are pink and Cu(II) species are navy blue in solution (at $\sim 10^{-5}$ M).

4. Cyclic voltammetry

To evaluate the influence of the central metal on the electronic structure of the macrocycle we decided to perform cyclic voltammetry on the Zn(II), Cu(II) and Pd(II) chlorins and compare them to their free base analogues. Results are summarized in Tables 2–4. Typical voltammograms are shown in Fig. 2, and all voltammograms are provided in the Supporting information. Voltammograms of the free base 10-furyl and 10-thienyl-chlorins have been reported before [14].

Table 2
Cyclic voltammetry data for free base chlorins.

Chlorin	Reduction, E _{pc} [V]		Oxidation, E _{pa} [V]	
	1	2	1	2
1a	−2.13	−1.71	0.43	0.99
1c	−2.16	−1.75	0.39	0.95
1e	−2.12	−1.71	0.46	0.98
1i	−2.11	−1.70	0.47	0.98
1b	−2.15	−1.69	0.44	0.98
1f	−2.23	−1.82	−1.69	−1.53
1j	−2.19	−1.72	0.40	0.93
1g	−2.20	−1.78	0.38	0.91
1k	−2.04	−1.60	0.53	0.99
1d	−2.11 ^a	−1.67 ^a	0.43 ^a	0.94 ^a
1h	−2.14 ^a	−1.67 ^a	0.43 ^a	0.83 ^a
1l	−2.14	−1.74	0.42	0.98

Measured for 1 mM solutions of the analyte in CH₂Cl₂ (0.1 M NBu₄PF₆), glassy C-electrode, $n = 100$ mV s^{−1}. All potentials are given versus Fc^{+/0}.

^a From reference [14].

All free base chlorins with electrochemically inert substituents (**1a**, **e**, **g**, **i**, **j** and **l**) show two oxidation and two reduction peaks, of which only the first reduction peak is reversible (Table 2). The macrocycle-based redox processes were assigned based on the similarities between the compounds. For example, phenyl-substituted **1a** had two oxidation and two reduction peaks, at 0.43 and 0.99 eV, and −1.71 and −2.13 eV, respectively. These values are almost identical to those obtained for the regioisomeric 15-phenyl chlorin [48]. The first oxidation potentials are somewhat substituent-dependent, and are in the 0.39–0.51 eV range. The separation between the first and the second oxidations are essentially constant in this series of chlorins, with a value of ~ 0.52 eV. The majority of the other chlorins studied here had similar peaks in the

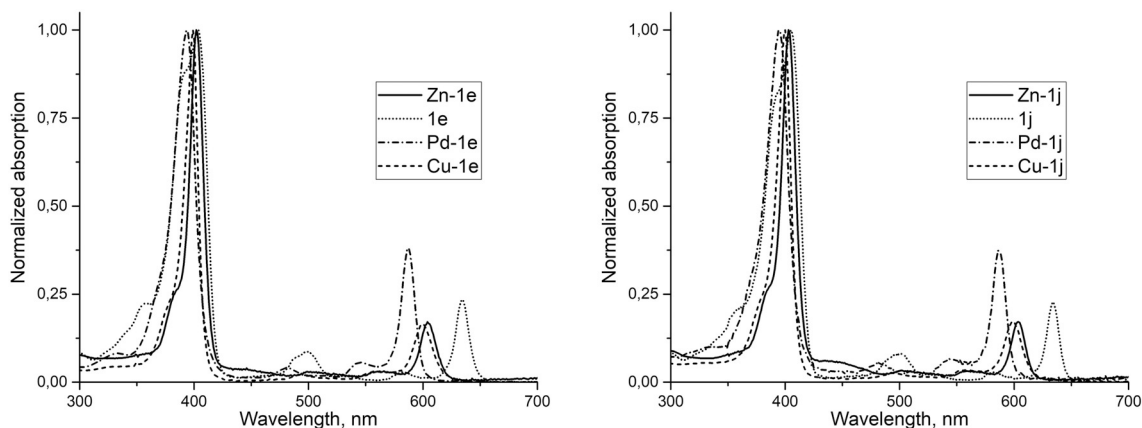


Fig. 1. Typical UV–Vis spectra of free base, Zn, Pd and Cu chlorins (**M-1e** (left) and **M-1j** (right)).

Table 3
Cyclic voltammetry data for Zn chlorins.

Chlorin	Reduction, E _{pc} [V]				Oxidation, E _{pa} [V]	
Zn-1a	-2.27	-1.87			0.148	0.605
Zn-1c	-2.32	-1.89			0.132	0.581
Zn-1e	-2.26	-1.85			0.173	0.606
Zn-1i	-2.25	-1.84			0.173	0.616
Zn-1b	-2.28	-1.84			0.183	0.616
Zn-1f	-2.28	-1.98	-1.55		0.220	0.66
Zn-1j	- ^a	- ^a	- ^a	- ^a	- ^a	- ^a
Zn-1g	-2.33	-1.87	-1.53	-1.08	0.138	0.56
Zn-1k	-2.15	-1.75			0.243	0.787
Zn-1d	-2.24	-1.81			0.183	0.621
Zn-1h	-2.26	-1.86			0.223	0.675
Zn-1l	-2.27	-1.90			0.148	0.60

Measured for 1 mM solutions of the analyte in CH₂Cl₂ (0.1 M NBu₄PF₆), glassy C-electrode, n = 100 mV s⁻¹. All potentials are given vs Fc^{+ / 0}.

^a Could not be determined due to instrument problems.

same region. There were a handful of exceptions to this pattern. Nitrophenyl-substituted **1f** showed additional reductions. These could tentatively be assigned to the stepwise reduction of the NO₂ group. Arylnitro compounds are known to undergo multielectron reductions via the nitroso species to the amine [49].

The voltammograms of the Zn(II) complexes were similar in shape to those of the free base substances, however all peaks except for the one corresponding to the second reduction became reversible. Both oxidations are happening at lower potentials, as expected for formally dianionic ligands (0.13–0.24 eV for first oxidation and 0.58–0.79 eV for the second). The oxidation potentials are correlated with the electronic properties of the substituent. Reductions are taking place at slightly (~0.1 eV) lower potentials than in the free base compounds, in line with the increased electron density of the macrocycle (Table 3). The reduction of nitrophenylchlorin **Zn-1f** was complicated, similarly to that of its free base analogue **1f**. 2,6-Dimethoxyphenyl-substituted **Zn-1g** showed two additional fully reversible reductions at -1.53 and -1.08 eV, the source of which is unclear at this point.

Pd(II) chlorins show two oxidation peaks appearing at almost the same potentials as the free base compounds, the first of these is reversible. Two reductions take place at -1.8 eV and -2.35 eV. The first one is located at a potential ~0.20 eV lower than the potential of the corresponding free base chlorin, and second is shifted by ~0.3 eV.

The oxidations of the Cu(II)-chlorins contained an additional, presumably metal-based oxidation peak. Of the three oxidation peaks only the first one was reversible. The first oxidation takes place at ~0.22 eV, which is located at ~0.20 eV lower potential than for the corresponding free base chlorins. Reduction potentials were almost identical to those of the analogous Pd(II) complexes, with electron transfers occurring between -1.86 and -2.40 eV for all 5 compounds tested. The effects of the 10-substituents on the macrocycle-based oxidation and reduction potentials follow the trends expected based on their electronic properties (vide infra). Interestingly, 2,6-dimethoxyphenyl-substituted **Cu-1g** and **Pd-1g** displayed reduction waves that were similar to those of Pd and Cu chelates carrying other substituents. We do not have an

Table 4
Cyclic voltammetry data for copper and palladium chlorins.

10-substituent	Cu chlorins				Pd chlorins				
	Reduction, E _{pc} [V]		Oxidation, E _{pa} [V]		Reduction, E _{pc} [V]		Oxidation, E _{pa} [V]		
Ph		-1.86	0.22	0.81	1.14	-2.34	-1.80	0.39	1.03
<i>p</i> -F-C ₆ H ₄	-2.38	-1.84	0.24	0.83	1.17	-2.32	-1.77	0.40	1.04
<i>p</i> -OCH ₃ -C ₆ H ₄	-2.39	-1.86	0.22	0.83	1.11	-2.36	-1.79	0.38	1.03
2,6-(OMe) ₂ -C ₆ H ₃	-2.43	-1.89	0.18	0.77	1.06		-1.86	0.34	1.04
<i>p</i> -OCH ₂ C(O)O ^t Bu-C ₆ H ₄	-2.38	-1.85	0.23	0.82	1.08	-2.35	-1.82	0.32	0.93

Measured for 1 mM solutions of the analyte in CH₂Cl₂ (0.1 M NBu₄PF₆), glassy C-electrode, n = 100 mV s⁻¹. All potentials are given versus Fc^{+ / 0}.

explanation for this result, however, it may reflect an increased macrocycle rigidity caused by metal ion coordination. This, in combination with the fact that the bulky 2,6-dimethoxyphenyl substituent is forced to be perpendicular to the macrocycle results in a diminished substituent-macrocycle communication compared to what is possible in the free base species. Further studies are required to understand the redox behavior of **M-1g**.

5. NMR spectroscopy

The electron density of the macrocycle is a known factor in determining metallochlorin stabilities. We investigated whether a meaningful correlation could be detected between chelate stability and the shielding of the macrocycle protons as observed in the ¹H NMR spectrum. If confirmed, this would provide a simple tool for the preliminary assessment of metallochlorin robustness. Therefore, the ¹H and ¹³C NMR spectra of all the diamagnetic chlorins were fully assigned using a combination of literature data, and ¹H-¹H correlation spectroscopy (COSY), attached proton test (APT) and heteronuclear single-quantum correlation spectroscopy (HSQC) experiments. Results are summarized in Figs. 3 and 4. Full spectra are provided in the Supporting Information. The aromatic regions of representative ¹H NMR spectra for the diamagnetic free base **1j** and Zn(II)- and Pd(II)-**1j** chlorins are shown in Fig. 3. These values are similar to those reported by Lindsey and co-workers [45,50,51] and Ptaszek et al. [7,11]. The Cu(II) chelates were paramagnetic, as expected [33,52].

Macrocycle resonances are in the range 8.5–10 ppm for deshielded β-pyrrolic C-H and meso C-H protons, and -1.8 ppm to -2.5 ppm for the shielded N-H protons. No obvious correlation between the nature of the 10-substituent and size of the chemical shift changes for the nearest 8-H and 12-H were found. This may be because the shift is due to a combination of electronic effects and a shielding by the 10-position aromatic ring in semi-perpendicular orientation. The N-pyrrolic protons in the free base chlorins were on the other hand very sensitive to 10-substitution. Their chemical shifts correlate strongly with electronic properties of the substituent expressed by the Hammett constant (Fig. S1).

Metalation influences the ¹H NMR signature [53]. Metal ion coordination shifts all macrocyclic signals upfield, with Δδ the largest for the meso protons (~0.4 ppm) and ~0.2 ppm for the β-pyrrolic protons. The size of the shift is metal ion dependent. On average, the largest upfield shifts were observed for Zn(II) complexes and moderate ones for Pd(II) (Table S3). This is in line with both the cyclic voltammetry data and the larger electronegativity of Pd. Substituent effects on the shifts of ¹H and ¹³C resonances of the meso-protons in the Pd chlorins was very small, < 0.4 ppm (Table S3).

6. Demetallation kinetics

With the full characterization in hand, the demetallation kinetics under acidic conditions was studied. Reactions were followed by UV-Vis absorption spectroscopy. Representative spectral changes in the red region of the spectrum for metallochlorins in CH₂Cl₂

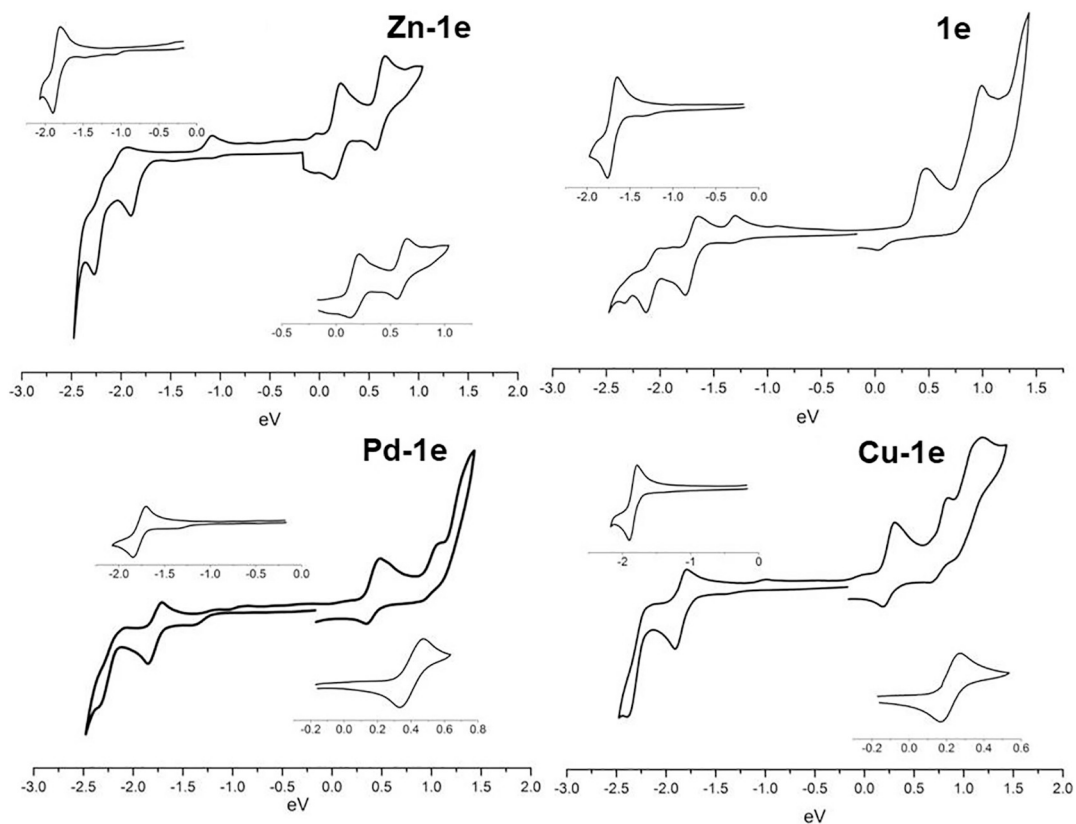


Fig. 2. Representative cyclic voltammograms for M-1e chlorins. All cyclic voltammograms are provided in the Supporting Information.

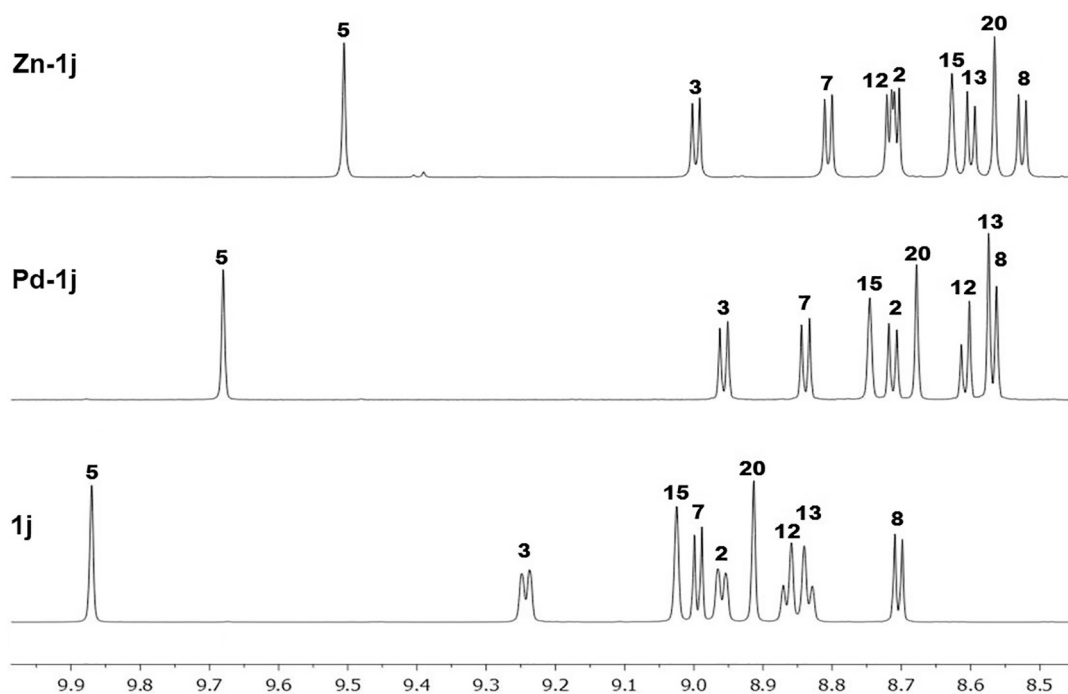


Fig. 3. Representative aromatic region of the ^1H NMR spectrum of M-1j chlorin in CDCl_3 .

([Chlorin] $\sim 8 \times 10^{-6}$ M) upon TFA addition ([TFA] $\sim 3 \times 10^{-2}$ M) are shown in Fig. 5. Similar spectra for the other metallochlorins are given in the Supporting Information (Figs. S70–78). It is important to note that the Zn(II) chelates were stable in solution in the absence of acid, and they could even be purified by column chromatography on mildly acidic silica gel. This increased stability compared to Mg(II)

chlorins facilitated the investigation of their demetallation kinetics.

Investigations began with the Zn(II) chelates, as these are known to undergo quantitative demetallation upon TFA-treatment on time scales ranging from minutes to hours. In the presence of a large excess of acid (pseudo first order conditions) the Soret band of the Zn(II) chlorin gradually disappeared, and a new, bathochromically shifted band

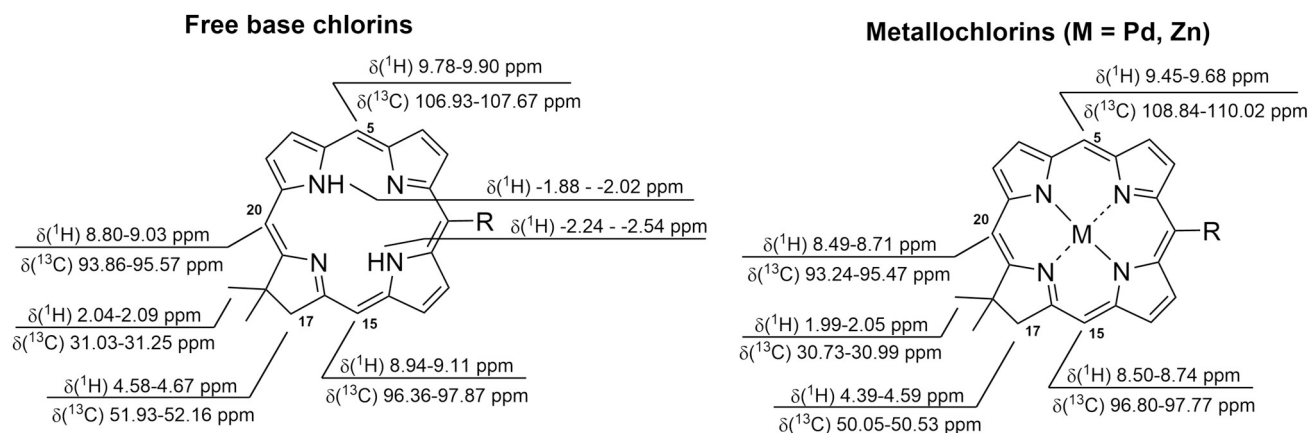


Fig. 4. Summary of ^1H NMR resonances of the free based and metallochlorins in CDCl_3 .

emerged. Similar trends are seen for the Q_y band at 604 nm, however, the change here is less pronounced as the bands overlap. Complexes **Zn-1a-e** and **Zn-1g-j** lost the Zn(II) within minutes. For compound **Zn-1k**, several hours were required for the same result, while the demetallation of **Zn-1f** was incomplete even after 12 h.

The reaction intermediates and products were identified by comparisons of the absorption maxima with those of well-characterized reference compounds. We have recently isolated and fully characterized three mono- and diprotonated free base chlorins (10-substituents: Ph, pentafluorophenyl, *p*-C₆H₄-OMe) [46]. With the help of these data we could identify the starting Zn(II) chlorin ($\lambda = 604$ nm for Ph), the charge-neutral free base chlorin ($\lambda = 633$ nm), the monoprotonated free base chlorin intermediates ($\lambda = 613$ nm). The overlaid UV-Vis traces of the reaction mixture during the demetallation and independently obtained reference compounds are presented in Fig. 5.

The mechanism of acidic demetallation of porphyrins and chlorins has been studied before [54-57]. Based on previous reports, as well as the species we could identify in the reaction mixtures, we have adopted the two-step sequence shown in Scheme 2 as the putative mechanism. The first step is demetallation of the starting metallochlorin (reaction rate k_1) to form free base chlorin. Most probably this step includes multiple steps, such as the coordination of the proton to the metallochlorin and expulsion of the metal (here: Zn²⁺) cation upon the arrival of the second proton. Based on the UV-Vis data reported herein we could not identify any of those intermediates and so assume them to be very short lived and not to be present in the reaction mixture in high enough concentration to be detected. Fukuzumi et al. have characterized several protonated Co(II) chlorins; however, protonation in these pyropheophorbide-derived chelates took place on the E-ring carbonyl oxygen [21,22]. It is worth noting that even at this remote site, basicity was greatly influenced by the electronic properties of the 3-substituents in the A-ring [21]. Subsequent protonation of free base chlorin leads to the formation of the singly N-protonated chlorin (reaction rate k_2). We have recently isolated and fully characterized such a species, and have shown that it is surprisingly stable under a range of conditions [46]. Therefore, it is reasonable to postulate the formation of a monoprotonated intermediate under these acidic solutions. The second step of the sequence presented in Scheme 2 was studied in detail. The values of k_2 correlated with the *para*-Hammett constants of the substituent in 10-position of the chlorin [46].

Since key intermediates (Zn chelate, free base and monoprotonated free base chlorin) have characteristic absorptions, quantitative analysis of the demetallation could be performed by following the absorbance changes. The concentrations of the intermediates were calculated from the absorption spectrum of the reaction mixture and the individual absorption spectra using a least square root method. After the completion of the reaction the UV-Vis absorption of the mixture resembled the spectrum of the monoprotonated free base chlorin (Fig. 5, middle).

This lends support to the process delineated in Scheme 2, ending in the monoprotonated free base chlorin. The free base chlorin and the monoprotonated free base chlorin are both downstream of the rate determining step (k_1). The absorption spectrum of the free base chlorin could be observed in the reaction mixture, however with a very low intensity. The rate constant of the free base chlorin protonation (k_2) could not be determined under these conditions.

The calculated rate constants for the formation of the free base chlorins (k_1) are summarized in Table 5. Initial protonation of the starting Zn(II) complexes is very fast, and is instantaneous under conditions that feature a large excess of the acid. The reaction rate for the first step is in the 1.0×10^{-3} to $1.29 \times 10^{-3} \text{ min}^{-1}$ range, with the exception of the least basic *p*-nitrophenyl and pentafluorophenyl-substituted complexes ($k_1 = 7.89 \times 10^{-5}$ and $1.92 \times 10^{-4} \text{ min}^{-1}$ respectively). This translates to a demetallation 47 times faster for Zn(II) chlorin with a *p*-methoxyphenyl substituent than with a *p*-nitrophenyl. In practice, the reaction mixture containing *p*-OMe contains < 1% of the starting Zn(II) complex after 10 min, while for the *p*-nitrophenyl compound after the same time 88% of the starting material remains (Table 6).

The pK_a values of the first protonation of the free base chlorin were estimated for the chlorins shown in Table 5. These values are similar to the ones determined previously for the **1a**, **1j** and **1k** chlorins. The macrocycle basicities vary with the electron-donating or withdrawing ability of the 10-substituent. The range of pK_a values is relatively modest, the most basic macrocycle (**1j**) has pK_a = 5.39, while the least basic (**1k**) pK_a = 4.79. Previously, we have noted good correlation between the Hammett constant of the 10-substituent and the pK_a of the first protonation of the free base chlorin [46], here, we relied on this observation to estimate the pK_a values in order to be able to extract the rate constants. The fastest demetallation was seen for the most basic macrocycle, while the slowest kinetics was noted in those carrying strongly electron-withdrawing groups (**1f**, **1k**). However, basicity correlates only loosely with the demetallation rate, and it appears that there are additional factors also in play, such as the different macrocycle distortions during protonation and metallation. The flexibility of the chlorin ligand conferred stability on the Co chelate of a pheophorbide under acidic conditions, while under the same conditions the Co complex of octaethylporphyrin was quantitatively demetallated [22]. Therefore, structural and electronic considerations are likely both important.

To see if the electronic properties of the macrocycle substituent correlate with the reaction rate, k_1 was plotted vs Hammett constants for the entire substituent on the macrocycle (Fig. 6). While slower kinetics was observed for the less electron-rich ligands, no linear dependence was obtained. This further suggests that the reaction is more complex and the demetallation is influenced by more than just electron-withdrawing/donating properties of the substituent present in the 10-

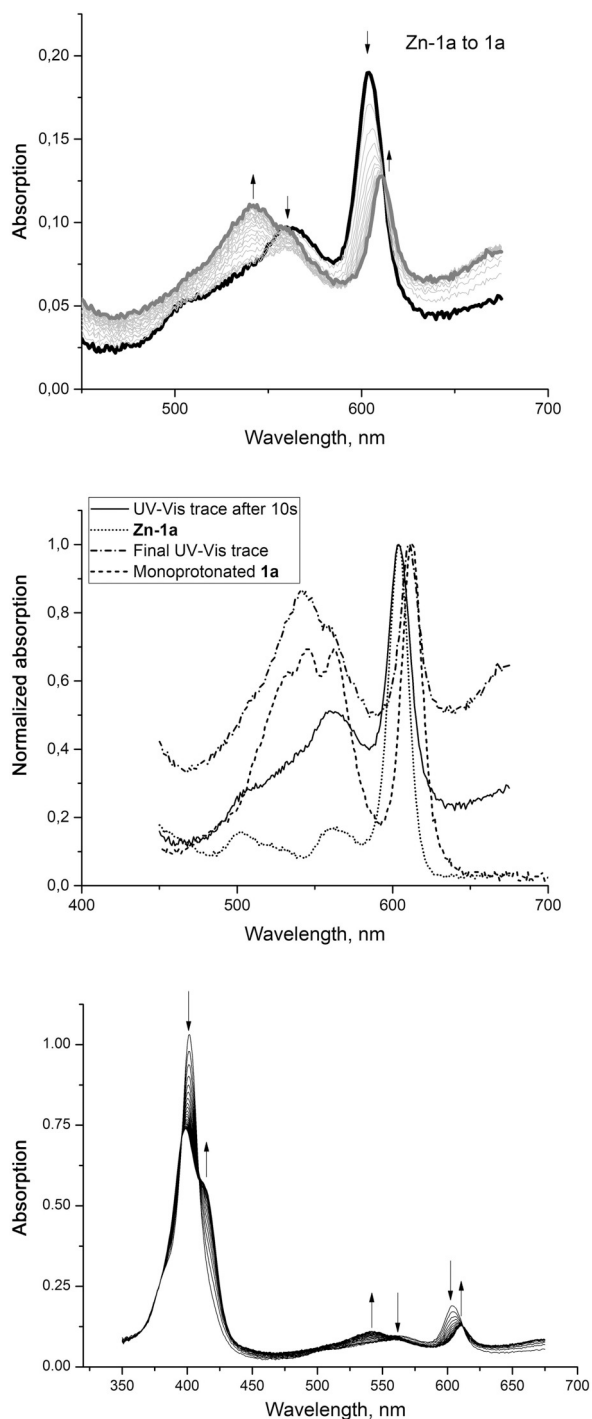
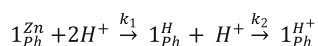


Fig. 5. Top: example of the experimental absorption changes during the demetallation reaction for **Zn-1a** to **1a**. Initial UV-Vis trace shown in black, the final spectrum after the reaction in dark grey. Middle: initial and final spectra of the reaction mixture overlaid with the UV-Vis traces of reference compounds. Bottom: Change of UV-Vis spectra during course of the demetallation reaction of **Zn-1a** (30 min). All data were normalized to simplify the figure.



Scheme 2. Demetallation mechanism used in the analysis of the data.

position of the macrocycle.

Finally, with the rate constants in hand, we note that the ^1H and ^{13}C NMR chemical shifts and the macrocycle oxidation and redox potentials

Table 5
Calculated reaction rates for demetallation of Zn chlorins.

		σ , 4-Ph-R	$k_1 \times 10^3$, min^{-1}	$\text{p}K_1$
1	Zn-1a	-0.01	1	5.27
2	Zn-1c	- ^a	- ^a	- ^a
3	Zn-1e	0.06	1.06	5.15
4	Zn-1i	0.12	1.08	5.05
5	Zn-1b	0.1	1.29	5.08
6	Zn-1f	0.26	0.0789	4.81
8	Zn-1j	-0.08	3.7	5.39
9	Zn-1g	- ^a	- ^a	- ^a
10	Zn-1k	0.27	0.192	4.79
11	Zn-1d	0.05	1.15	5.17
12	Zn-1h	0.02	1.13	5.22

^a Not determined because Hammett constants were not available for substituent.

Table 6
Proportion of Zn(II) complexes carrying different 10-substituents in the reaction mixtures at the different time points.

	Zn-1j	Zn-1a	Zn-1f
10 min	< 1%	27%	88%
30 min	-	< 1%	73%
5 h	-	-	< 4%

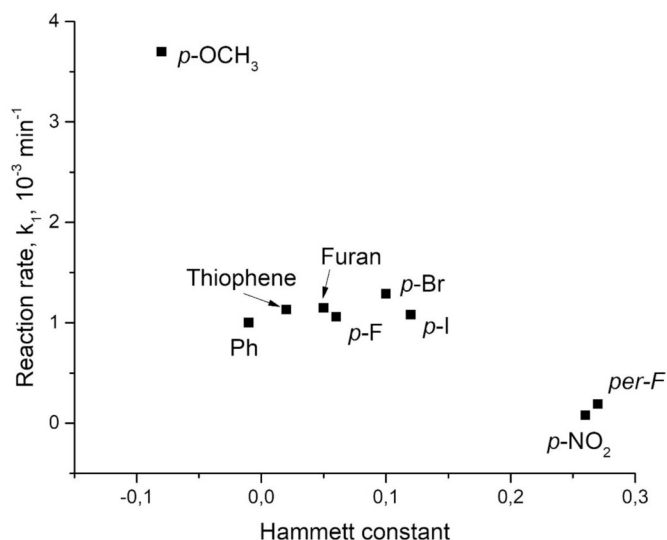


Fig. 6. Correlation of the Hammett constants vs. calculated demetallation rate k_1 .

are, with one possible exception, unhelpful in predicting Zn(II) chlorin stability. The exceptions are the N-H resonances, which showed good correlation for the set of free base chlorins analyzed with the *meso*-substituent's Hammett constants, and with sufficiently large differences. As the demetallation rates loosely correlated with the substituent Hammett constants, the inner N-H resonance could be a good initial guide to stability. Calculations by Holten, Bocian and Lindsey on Zn chlorins carrying 0-4 *meso*-substituents showed that the highest occupied molecular orbital-1 (HOMO-1) orbital has large coefficients on the *meso*-positions, the nitrogens and the central Zn, suggesting the presence of high electron density on these positions. Helaja et al. have calculated electron density maps for a series of chlorin tautomers. They found that in the most stable *trans*-N21-H,N23 tautomer electron density is highest in the *meso*-positions and on the nitrogen atoms [58]. In the absence of blocking substituents chlorins react with electrophiles in the *meso*-positions [59-61]. These data are all consistent with the observation that the *meso*-substituent strongly impacts the electronic

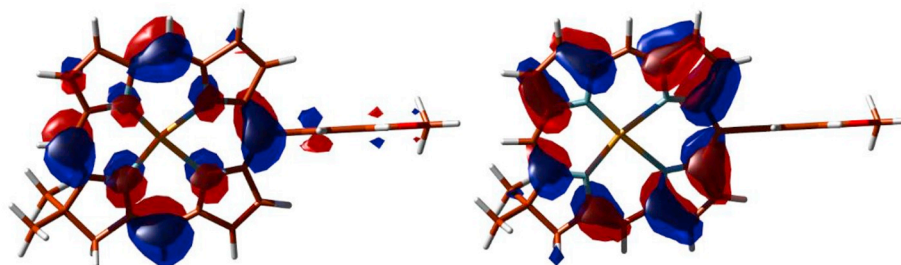


Fig. 7. HOMO-1 and HOMO of Zn-1j.

properties of the macrocycle. The HOMO on the other hand had no contributions from the meso-carbons [62]. This is analogous to what has been seen in free base chlorins. The 10-*p*-methoxyphenyl-substituent also has a small contribution to the HOMO-1, seen both in the free base and the Zn chelate (Fig. 7) [46].

The analysis of the Pd(II) and Cu(II) chlorin demetallation kinetics will be the subject of subsequent investigations. However, the current work was prompted by the high acid sensitivity of Cu-11, and we note that the Zn analogue of the electronically similar 1j displayed very fast demetallation kinetics. Therefore, we expect that for Cu(II) and Pd(II) the findings on Zn(II) chlorins will be mirrored.

7. Conclusion

A library of synthetic metallochlorins varying only in their 10-substituent was demetallated under acidic conditions. The rate of the loss of the metal was analyzed using UV-Vis absorption spectroscopy. By comparison of the absorption spectra of the reaction mixtures with authentic samples of free base and metallochlorins, as well as those of monoprotonated chlorins obtained under controlled conditions we were able to extract pseudo first-order rate constants. The rate of demetallation was faster for more basic chlorins, which is expected. This observation is also in line with previous literature reports.

Somewhat more surprisingly, we measured rate constants that varied by orders of magnitude in chlorins that differed only in a single substituent in the *p*-position of a 10-phenyl group. Currently, it is not known whether groups in all other peripheral positions provide similar levels of control over the properties of the macrocycle. Previously, Saga and co-workers have noted a 20-fold acceleration upon replacement of the 3-vinyl group with an acetyl. These groups were directly attached to the macrocycle, so the effect seems smaller than in the systems investigated herein. However, the difference in reaction conditions (solvents) precludes the direct comparison of the data [28]. Our results suggest that the stabilities of the increasingly utilized metallochlorins could be readily tuned by the judicious choice of quite remote functionalities.

8. Experimental

8.1. General

All reactions were performed under and Ar atmosphere using Schlenk techniques unless stated otherwise. Diethyl ether and THF were freshly distilled from Na/benzophenone prior to use. CH₂Cl₂ was distilled from CaH₂. ¹H and ¹³C spectra were recorded on a 400 MHz spectrometer. Chemical shifts (ppm) are reported and referenced to the internal signal of residual solvent protons. High resolution mass spectral analyses (HRMS) were performed at the Organisch Chemisches Institut of the University of Münster on a high resolution FTMS + pNSI mass spectrometer (OrbitrapXL).

Calculations. All calculations were performed with the Gaussian suit of programs (G09 Rev. C.01) [63]. All structures were fully optimized using the MO6-2X functional with a 6-311 + +G** basis set which

proved suitable for accurate calculation of large π -conjugated systems. Structures were determined to be true minima by performing a vibrational analysis. Geometries and electron densities were analyzed and visualized using Molden [64].

General procedure for preparation of Zn-chlorins: Chlorins were prepared following the general procedure developed by Lindsey [37,39]. Compounds Zn-1a, c [39,43], Zn-1d [14], Zn-1f [44], Zn-1g [45], Zn-1h [14], Zn-1j [46], Zn-1k [46], Zn-1l [33], Pd-1a,l [33] and Cu-1a,l [33,39] were synthesized following literature procedures. Their characterization data were in accordance with reported values. Synthesis of macrocycles consists of two steps – bromination of the corresponding formyldipyrromethane and macrocyclisation itself. Due to low solubility of the 1-bromo-9-formyldipyrromethane, bromination was usually performed directly before cyclisation, and the product was used in the subsequent steps without further purification.

Step 1. Bromination. A sample of 1-formyldipyrromethane (1 equiv.) dissolved in dry THF was cooled to -78°C . The solution was treated dropwise with a THF-solution containing 1 equiv. of NBS. The reaction mixture was stirred for 30 min, during which time it was allowed to slowly warm up to approximately -50°C . The reaction was quenched by the addition of 30 mL brine, and the mixture was allowed to warm up to room temperature. After this two phases are separated and aqueous layer extracted with 2×50 mL of diethyl ether. Combined organic layers are washed with 50 mL of brine and dried over MgSO₄. Removing of the solvent under reduced pressure (Caution! temperature of the water bath should not be $> 25^{\circ}\text{C}$) gives crude product which is directly used in the next step without additional purification.

Step 2. Macrocyclisation. Manipulations should be performed with the exclusion of light. To the solution of bromoformyldipyrromethane (1 equiv.) and Western half (1 equiv.) in dry CH₂Cl₂ solution of 5 equiv. of *p*-toluenesulfonic acid monohydrate in MeOH was added. The reaction mixture was stirred for 30 min, and the reaction was then quenched by the addition of 10 equiv. of TMPP. Solvents were removed under reduced pressure. The temperature of the water bath should not exceed 25°C . The solid residue was dissolved in dry acetonitrile. TMPP (25 equiv.), Zn(OAc)₂ (15 equiv.) and AgOTf (3 equiv.) were added, and the reaction mixture was heated at reflux for 16–24 h in the dark and open to the air. During this time a dark gray to black suspension formed. Filtration through a silica pad and thorough washing with CH₂Cl₂, followed by the evaporation of the solvents from the filtrate gave dark green to black crude products. Column chromatography on silica gel using 50% CH₂Cl₂ in hexane gave spectroscopically clean products as dark green solids after solvent evaporation.

8.2. Zn-1b

Bromination was performed starting from 80 mg (0.21 mmol) of the required dipyrromethane and 38 mg (0.21 mmol) of NBS. During macrocyclization 39 mg (0.21 mmol) of Western half, 200 mg (1.05 mmol) of *p*-toluenesulfonic acid monohydrate, 296 mg (2.10 mmol) and 740 mg (5.25 mmol) of TMPP, 576 mg (3.15 mmol) of Zn(OAc)₂ and 162 mg (0.63 mmol) of AgOTf were used. R_f (50% CH₂Cl₂ in hexane) = 0.48. Yield: 19%, 24 mg.

^1H NMR (400 MHz, CDCl_3): δ = 9.58 (s, 1H), 9.06 (d, J = 4 Hz, 1H), 8.84 (d, J = 4 Hz, 1H), 8.77 (d, J = 4 Hz, 1H), 8.69 (s, 1H), 8.65 (d, J = 5 Hz, 1H), 8.63 (d, J = 5 Hz, 1H), 8.62 (s, 1H), 8.47 (d, J = 4 Hz, 1H), 8.47 (d, J = 4 Hz, 1H), 8.04 (d, J = 8 Hz, 2H), 7.81 (d, J = 8 Hz, 2H), 4.52 (s, 2H), 2.04 (s, 6H) ppm. ^{13}C NMR (101 MHz, CDCl_3): δ = 171.2, 159.4, 154.1, 153.2, 146.8, 146.5, 146.1, 145.5, 142.0, 135.8, 135.4, 133.1, 132.8, 128.8, 128.2, 127.5, 127.0, 122.0, 109.5, 97.1, 94.4, 93.6, 50.3, 45.4, 31.0 ppm. HRMS: calc. $\text{C}_{28}\text{H}_{21}\text{N}_4\text{Zn}$ $[\text{M}]^+$ 604.0097, obsd. 604.0075.

8.3. Zn-1e

Bromination was performed using 343 mg (1.30 mmol) of the required dipyrromethane and 228 mg (1.30 mmol) of NBS. During macrocyclisation 244 mg (1.30 mmol) of Western half, 1.24 g (6.50 mmol) of *p*-toluenesulfonic acid monohydrate, 1.83 g (13.0 mmol) and 4.58 g (32.5 mmol) of TMPP, 3.57 g (19.5 mmol) of $\text{Zn}(\text{OAc})_2$ and 1.002 g (3.9 mmol) of AgOTf were used. R_f (50% CH_2Cl_2 in hexane) = 0.49. Yield: 16.8%, 110 mg. ^1H NMR (400 MHz, CDCl_3): δ = 9.58 (s, 1H), 9.06 (d, J = 4 Hz, 1H), 8.84 (d, J = 4 Hz, 1H), 8.77 (d, J = 4 Hz, 1H), 8.69 (s, 1H), 8.64 (d, J = 5 Hz, 2H), 8.62 (s, 1H), 8.47 (d, J = 4 Hz, 1H), 8.03 (dd, J = 9, J_{HF} = 6 Hz, 2H), 7.40 (dd, J = 9, J_{HF} = 9 Hz, 2H), 4.52 (s, 2H), 2.04 (s, 6H) ppm. ^{13}C NMR (101 MHz, CDCl_3): δ = 171.2 (s), 163.9 (s), 161.4 (s), 159.3 (s), 154.1 (s), 153.1 (s), 147.2 (s), 146.5 (s), 146.0 (s), 138.3 (d, J = 3 Hz), 134.9 (d, J = 8 Hz), 133.0 (s), 132.9 (s), 128.8 (s), 128.2 (s), 127.4 (s), 126.8 (s), 122.30 (s), 113.6 (d, J = 21 Hz), 109.4 (s), 97.0 (s), 94.4 (d, J = 17 Hz), 50.3 (s), 45.4 (s), 30.9 (s) ppm. HRMS: calc. $\text{C}_{28}\text{H}_{21}\text{FN}_4\text{Zn}$ $[\text{M}]^+$ 496.1036, obsd. 496.1022.

8.4. Zn-1i

Bromination was performed starting from 33 mg of the required, 18 mg of NBS. During macrocyclisation 19 mg of Western half, 95 mg of *p*-toluenesulfonic acid monohydrate, 141 mg and 352 mg of TMPP, 274 mg of $\text{Zn}(\text{OAc})_2$ and 77 mg of AgOTf were used. R_f (50% CH_2Cl_2 in hexane) = 0.37. Yield: 21%, 12 mg.

^1H NMR (400 MHz, CDCl_3): δ = 9.62 (s, 1H), 9.09 (d, J = 4 Hz, 1H), 8.86 (d, J = 4 Hz, 1H), 8.78 (d, J = 4 Hz, 1H), 8.71 (s, 1H), 8.65 (s, 1H), 8.65 (s, 1H), 8.63 (s, 1H), 8.48 (d, J = 4 Hz, 1H), 7.94 (d, J = 8 Hz, 2H), 7.82 (d, J = 8 Hz, 2H), 4.53 (s, 2H), 2.03 (s, 6H) ppm. ^{13}C NMR (101 MHz, CDCl_3): δ = 171.3, 159.6, 154.2, 153.3, 146.7, 146.2, 141.5, 135.1, 133.2, 132.9, 129.9, 128.9, 128.4, 127.6, 127.1, 122.0, 109.5, 97.2, 94.4, 50.4, 45.5, 31.0 ppm. HRMS: calc. $\text{C}_{28}\text{H}_{21}\text{BrN}_4\text{Zn}$ $[\text{M}]^+$ 558.0215, obsd. 558.0227.

General procedure for the preparation of free base chlorins from Zn chlorins: To the solution of the Zn chlorin in 50 mL of dry CH_2Cl_2 ca. 0.25 mL of TFA was added in one portion. The reaction mixture was stirred at room temperature for 20 min. The reaction was quenched with 1 mL of triethylamine. The resulting dark green to black solution was then directly applied onto a silica gel column. The product was eluted with 50% CH_2Cl_2 in hexane mixture. Removal of the solvent under reduced pressure gave spectroscopically clean products as dark green solids.

8.5. 1b

Reaction was performed using 13 mg (0.021 mmol) of Zn chlorin. R_f (50% CH_2Cl_2 in hexane) = 0.47. Yield: 64%, 7.3 mg.

^1H NMR (400 MHz, CDCl_3): δ = 9.88 (s, 1H), 9.26 (d, J = 5 Hz, 1H), 9.06 (s, 1H), 8.99 (d, J = 4 Hz, 1H), 8.97 (s, 1H), 8.94 (s, 1H), 8.85 (d, J = 5 Hz, 1H), 8.80 (d, J = 5 Hz, 1H), 8.63 (d, J = 4 Hz, 1H), 4.66 (s, 2H), 2.08 (s, 6H), -2.00 (s, 1H), -2.37 (s, 1H) ppm. ^{13}C NMR (101 MHz, CDCl_3): δ = 175.4, 163.0, 152.0, 150.9, 141.3, 141.0, 139.5, 136.0, 135.8, 134.8, 134.3, 132.5, 131.7, 128.4, 127.9, 123.7,

123.3, 119.8, 107.3, 97.0, 94.4, 93.9, 52.0, 46.5, 31.2 ppm. HRMS: calc. $\text{C}_{28}\text{H}_{24}\text{IN}_4$ $[\text{M} + \text{H}]^+$ 543.1040, obsd. 543.1034.

8.6. 1e

Reaction was performed using 15.7 mg (0.032 mmol) of Zn chlorin. R_f (50% CH_2Cl_2 in hexane) = 0.45. Yield: 94%, 13.1 mg.

^1H NMR (400 MHz, CDCl_3): δ = 9.88 (s, 1H), 9.26 (d, J = 5 Hz, 1H), 9.06 (s, 1H), 8.99 (d, J = 4 Hz, 1H), 8.97 (d, J = 5 Hz, 1H), 8.93 (s, 1H), 8.85 (d, J = 5 Hz, 1H), 8.79 (d, J = 5 Hz, 1H), 8.62 (d, J = 4 Hz, 1H), 8.12 (dd, J = 9, J_{HF} = 6 Hz, 2H), 7.44 (dd, J = 9, J_{HF} = 9 Hz, 2H), 4.66 (s, 2H), 2.08 (s, 6H), -1.97 (s, 1H), -2.35 (s, 1H). ^{13}C NMR (101 MHz, CDCl_3): δ = 175.4 (s), 164.0 (s), 162.9 (s), 152.5 (s), 150.9 (s), 141.0 (s), 139.5 (s), 137.7 (d, J = 3 Hz), 135.3 (d, J = 8 Hz), 135.2 (d, J = 1 Hz), 134.2 (s), 132.4 (s), 131.8 (s), 128.4 (s), 128.0 (s), 123.6 (s), 123.3 (s), 120.1 (s), 113.8 (d, J = 21.4 Hz), 107.2 (s), 96.9 (s), 94.3 (s), 52.0 (s), 46.5 (s), 31.2 (s) ppm. HRMS: calc. $\text{C}_{28}\text{H}_{24}\text{FN}_4$ $[\text{M} + \text{H}]^+$ 435.1980, obsd. 435.1975.

8.7. 1i

Reaction was performed using 26 mg (0.046 mmol) of Zn chlorin. R_f (50% CH_2Cl_2 in hexane) = 0.53. Yield: 91%, 21 mg.

^1H NMR (400 MHz, CDCl_3): δ = 9.88 (s, 1H), 9.25 (d, J = 4 Hz, 1H), 9.06 (s, 1H), 9.00–8.95 (m, 2H), 8.94 (s, 1H), 8.85 (d, J = 5 Hz, 1H), 8.79 (d, J = 5 Hz, 1H), 8.61 (d, J = 4 Hz, 1H), 8.02 (d, J = 8 Hz, 2H), 7.87 (d, J = 8 Hz, 2H), 4.65 (s, 2H), 2.06 (s, 6H), -2.05 (s, 1H), -2.36 (s, 1H) ppm.

^{13}C NMR (101 MHz, CDCl_3): δ = 175.4, 163.0, 152.1, 150.9, 141.0, 140.7, 139.5, 135.5, 134.9, 134.9, 134.2, 134.2, 132.5, 131.7, 130.0, 128.4, 127.9, 123.7, 123.4, 122.2, 122.2, 119.7, 119.7, 107.3, 97.0, 94.4, 52.0, 46.5, 31.2. HRMS: calc. $\text{C}_{28}\text{H}_{24}\text{BrN}_4$ $[\text{M} + \text{H}]^+$ 495.1179, obsd. 495.1167.

General procedure for the preparation of Pd chlorins: To the solution of 1 equiv. of free base chlorin in 5 mL of pyridine, 5 equiv. of Pd (acac)₂ was added. The reaction mixture was irradiated in microwave reactor for 30 min at 180 °C. After the completion of the reaction the solvent was removed under reduced pressure, and the solid residue was extracted with CH_2Cl_2 . Column chromatography on silica gel using 50% CH_2Cl_2 in hexane gave spectroscopically clean products as bright pink solids after solvent removal.

8.8. Pd-1e

Reaction was performed using 15 mg (0.035 mmol) of free base chlorin. R_f (50% CH_2Cl_2 in hexane) = 0.58. Yield: 71%, 13.3 mg.

^1H NMR (400 MHz, CDCl_3): δ = 9.68 (s, 1H), 8.96 (d, J = 5 Hz, 1H), 8.84 (d, J = 5 Hz, 1H), 8.74 (s, 1H), 8.72 (d, J = 5 Hz, 1H), 8.69 (s, 1H), 8.57 (d, J = 5 Hz, 1H), 8.53 (d, J = 5 Hz, 1H), 8.49 (d, J = 5 Hz, 1H), 8.01 (dd, J = 8, J_{HF} = 6 Hz, 2H), 7.40 (dd, J = 8, J_{HF} = 9 Hz, 2H), 4.57 (s, 2H), 2.01 (s, 6H) ppm. ^{13}C NMR (101 MHz, CDCl_3): δ = 164.0 (s), 161.6 (s), 150.0 (s), 145.5 (s), 144.6 (s), 138.7 (d, J = 0.4 Hz), 138.4 (s), 137.6 (s), 137.4 (d, J = 3 Hz), 137.3 (s), 134.7 (d, J = 8 Hz), 132.0 (s), 131.8 (s), 127.5 (d, J = 16 Hz), 127.1 (s), 126.5 (s), 113.9 (s), 113.7 (s), 110.0 (s), 97.8 (s), 95.5 (s), 50.1 (s), 45.5 (s), 30.8 (s) ppm. HRMS: calc. $\text{C}_{28}\text{H}_{21}\text{FN}_4\text{Pd}$ $[\text{M}]^+$ 538.0790, obsd. 538.0770.

8.9. Pd-1g

Reaction was performed using 15 mg (0.031 mmol) of free base chlorin. R_f (50% CH_2Cl_2 in hexane) = 0.51. Yield: 69%, 12.4 mg.

^1H NMR (400 MHz, CDCl_3): δ = 9.66 (s, 1H), 8.94 (d, J = 5 Hz, 1H), 8.81 (d, J = 5 Hz, 1H), 8.72 (s, 1H), 8.69 (d, J = 5 Hz, 1H), 8.66 (s, 1H), 8.54 (s, 2H), 8.49 (d, J = 5 Hz, 1H), 7.67 (t, J = 8 Hz, 1H), 6.96 (d, J = 9 Hz, 2H), 4.57 (s, 2H), 3.52 (s, 6H), 2.01 (s, 6H) ppm. ^{13}C

NMR (101 MHz, CDCl₃): δ = 160.8, 160.2, 149.5, 145.0, 144.5, 139.3, 138.0, 137.9, 137.0, 131.4, 130.0, 127.5, 126.8, 126.5, 126.3, 119.1, 116.4, 109.9, 104.3, 97.4, 95.2, 56.1, 50.2, 45.4, 30.7 ppm. HRMS: calc. C₃₀H₂₆N₄O₂Pd [M]⁺ 580.1096, obsd. 580.1091.

8.10. Pd-1j

Reaction was performed using 21 mg (0.047 mmol) of free base chlorin. R_f (50% CH₂Cl₂ in hexane) = 0.57. Yield: 67%, 17 mg.

¹H NMR (400 MHz, CDCl₃): δ = 9.68 (s, 1H), 8.96 (d, *J* = 5 Hz, 1H), 8.84 (d, *J* = 5 Hz, 1H), 8.75 (s, 1H), 8.71 (d, *J* = 5 Hz, 1H), 8.68 (s, 1H), 8.61 (d, *J* = 5 Hz, 1H), 8.57 (d, *J* = 5 Hz, 2H), 8.57 (d, *J* = 5 Hz, 2H), 7.97 (d, *J* = 9 Hz, 2H), 7.23 (d, *J* = 9 Hz, 2H), 4.58 (s, 2H), 4.07 (s, 3H), 2.01 (s, 6H) ppm. ¹³C NMR (101 MHz, CDCl₃): δ = 161.5, 159.3, 149.8, 145.5, 144.6, 139.1, 138.4, 137.6, 137.5, 134.4, 133.8, 132.1, 131.9, 127.9, 127.3, 126.9, 126.2, 123.9, 112.3, 110.0, 97.7, 95.3, 55.5, 50.1, 45.5, 30.8 ppm. HRMS: calc. C₂₉H₂₄N₄OPd [M]⁺ 550.0990, obsd. 550.1018.

General procedure for the preparation of Cu chlorins: To the solution of 1 equiv. of free base chlorin in 15 mL of CH₂Cl₂ 5 equiv. of Cu (OAc)₂ was added. The reaction mixture was stirred at room temperature for 12 h. The mixture was directly applied onto a silica gel column. Elution with 50% CH₂Cl₂ in hexane gave spectroscopically clean products as bright turquoise solids after solvent removal.

8.11. Cu-1e

Reaction was performed using 25 mg (0.056 mmol) of free base chlorin. R_f (50% CH₂Cl₂ in hexane) = 0.51. Yield: 68%, 19 mg. HRMS: calc. C₂₈H₂₁N₄CuF [M]⁺ 495.1041, obsd. 495.1032.

8.12. Cu-1g

Reaction was performed using 15 mg (0.031 mmol) of free base chlorin. R_f (50% CH₂Cl₂ in hexane) = 0.32. Yield: 74%, 12.3 mg. HRMS: calc. C₃₀H₂₆N₄O₂Cu [M]⁺ 537.1346, obsd. 537.1341.

8.13. Cu-1j

Reaction was performed using 20 mg (0.045 mmol) of free base chlorin. R_f (50% CH₂Cl₂ in hexane) = 0.44. Yield: 53%, 12 mg. HRMS: calc. C₂₉H₂₄N₄OCu [M]⁺ 507.1241, obsd. 507.1225.

Abbreviations

acac	Acetylacetonate
APT	Attached proton test
COSY	Correlation spectroscopy
E _{pa}	Anodic potential
E _{pc}	Cathodic potential
Fc	Ferrocene
HOMO	Highest occupied molecular orbital
HRMS	High resolution mass spectrometry
HSQC	Heteronuclear single quantum coherence
I _B /I _Q	Ratio between the B and Q bands
NBS	N-bromosuccinimide
R _f	Retention factor
TFA	Trifluoroacetic acid
THF	Tetrahydrofuran
TMPP	2,2,6,6-tetramethylpiperidine

Declaration of competing interest

The authors declare that they have no known competing financial interests or personal relationships that could have appeared to influence the work reported in this paper.

Acknowledgments

This work was supported by the Swedish Research Council (project grant 2013-4655 to KEB), and Stiftelsen Olle Engkvist Byggmästare (post doc fellowship to A.I.A.).

Synthesis and characterization data for all new compounds. Cyclic voltammograms, ¹H and ¹³C NMR data and UV–Vis absorption spectra for new chlorins. UV–Vis absorptions of acidic demetallations. Supplementary data to this article can be found online at doi: <https://doi.org/10.1016/j.jinorgbio.2019.110979>.

References

- [1] M. Taniguchi, J.S. Lindsey, Chem. Rev. 117 (2017) 344–535.
- [2] J.S. Lindsey, Chem. Rev. 115 (2015) 6534–6620.
- [3] K.E. Borbas, in, World Scientific Publishing Co. Pte. Ltd., 2016, pp. 1–149.
- [4] S.K. Pandey, X. Zheng, J. Morgan, J.R. Missert, T.-H. Liu, M. Shibata, D.A. Bellnier, A.R. Oseroff, B.W. Henderson, T.J. Dougherty, R.K. Pandey, Mol. Pharm. 4 (2007) 448–464.
- [5] Z. Zheng, A. Graham, M. Shibata, J.R. Missert, A.R. Oseroff, T.J. Dougherty, R.K. Pandey, J. Org. Chem. 66 (2001) 8709–8716.
- [6] F. Rancan, A. Wiehe, M. Noebel, M.O. Senge, S.A. Omari, F. Boehm, M. John, B. Roeder, J. Photochem. Photobiol. B 78 (2005) 17–28.
- [7] N.N. Esemoto, A. Satraitis, L. Wiratan, M. Ptaszek, Inorg. Chem. 57 (2018) 2977–2988.
- [8] K. Lu, C. He, N. Guo, C. Chan, K. Ni, R.R. Weichselbaum, W. Lin, J. Am. Chem. Soc. 138 (2016) 12502–12510.
- [9] K. Lu, C. He, W. Lin, J. Am. Chem. Soc. 137 (2015) 7600–7603.
- [10] R. Xiong, D. Mara, J. Liu, R. Van Deun, K.E. Borbas, J. Am. Chem. Soc. 140 (2018) 10975–10979.
- [11] A. Meares, A. Satraitis, N. Santhanam, Z. Yu, M. Ptaszek, J. Org. Chem. 80 (2015) 3858–3869.
- [12] K.M. Faries, J.R. Diers, J.W. Springer, E. Yang, M. Ptaszek, D. Lahaye, M. Krayner, M. Taniguchi, C. Kirmaier, J.S. Lindsey, D.F. Bocian, D. Holten, J. Phys. Chem. B 119 (2015) 7503–7515.
- [13] F. Ogata, T. Nagaya, Y. Maruoka, J. Akhigbe, A. Meares, M.Y. Lucero, A. Satraitis, D. Fujimura, R. Okada, F. Inagaki, P.L. Choyke, M. Ptaszek, H. Kobayashi, Bioconjug. Chem. 30 (2019) 169–183.
- [14] R. Xiong, A.-B. Bornhof, A.I. Arkhynchuk, A. Orthaber, K.E. Borbas, Chem. Eur. J. 23 (2017) 4229.
- [15] R. Liu, J.S. Lindsey, ACS Macro Lett. 8 (2019) 154.
- [16] R. Liu, J.S. Lindsey, ACS Macro Lett. 8 (2019) 79–83.
- [17] G. Hu, H.S. Kang, A.K. Mandal, A. Roy, C. Kirmaier, D.F. Bocian, D. Holten, J.S. Lindsey, RSC Adv. 8 (2018) 23854–23874.
- [18] D.F. O'Shea, M.A. Miller, H. Matsueda, J.S. Lindsey, Inorg. Chem. 35 (1996) 7325–7338.
- [19] G.K. Lahiri, J.S. Summers, A.M. Stolzenberg, Inorg. Chem. 30 (1991) 5049–5052.
- [20] A.G. Maher, G. Passard, D.K. Dogutan, R.L. Halbach, B.L. Anderson, C.J. Gagliardi, M. Taniguchi, J.S. Lindsey, D.G. Nocera, ACS Catal. 7 (2017) 3597–3606.
- [21] K. Mase, K. Ohkubo, S. Fukuzumi, Inorg. Chem. 54 (2015) 1808–1815.
- [22] K. Mase, K. Ohkubo, S. Fukuzumi, J. Am. Chem. Soc. 135 (2013) 2800–2808.
- [23] M. Taniguchi, M. Ptaszek, B.E. McDowell, P.D. Boyle, J.S. Lindsey, Tetrahedron 63 (2007) 3850–3863.
- [24] O. Mass, M. Taniguchi, M. Ptaszek, J.W. Springer, K.M. Faries, J.R. Diers, D.F. Bocian, D. Holten, J.S. Lindsey, New J. Chem. 35 (2011) 76–88.
- [25] J.W. Springer, K.M. Faries, J.R. Diers, C. Muthiah, O. Mass, H.L. Kee, C. Kirmaier, J.S. Lindsey, D.F. Bocian, D. Holten, Photochem. Photobiol. 88 (2012) 651–674.
- [26] K. Sadaoka, Y. Hirai, S. Kashimura, Y. Saga, Chem. Lett. 39 (2010) 567–569.
- [27] Y. Saga, H. Tamiaki, Chem. Biodivers. 9 (2012) 1659–1683.
- [28] Y. Saga, R. Miura, K. Sadaoka, Y. Hirai, J. Phys. Chem. B 115 (2011) 11757–11762.
- [29] Y. Saga, Y. Hirai, K. Sadaoka, M. Isaji, H. Tamiaki, Photochem. Photobiol. 89 (2013) 68–73.
- [30] Y. Saga, A. Maruko, K. Sadaoka, N. Takahashi, Chem. Lett. 42 (2013) 672–674.
- [31] Y. Saga, Y. Kobashiri, K. Sadaoka, Inorg. Chem. 52 (2013) 204–210.
- [32] A.R. Battersby, K. Jones, R.J. Snow, Angew. Chem. 95 (1983) 742–743.
- [33] R. Xiong, J. Andres, K. Scheffler, K.E. Borbas, Dalton Trans. 44 (2015) 2541–2553.
- [34] Y. Saga, S. Hojo, Y. Hirai, Bioorg. Med. Chem. 18 (2010) 5697–5700.
- [35] G. Mackinney, M.A. Joslyn, J. Am. Chem. Soc. 63 (1941) 2530–2531.
- [36] G. Mackinney, M.A. Joslyn, J. Am. Chem. Soc. 62 (1940) 231–232.
- [37] M. Taniguchi, D. Ra, G. Mo, T. Balasubramanian, J.S. Lindsey, J. Org. Chem. 66 (2001) 7342–7354.
- [38] T. Balasubramanian, J.-P. Strachan, P.D. Boyle, J.S. Lindsey, J. Org. Chem. 65 (2000) 7919–7929.
- [39] M. Ptaszek, B.E. McDowell, M. Taniguchi, H.-J. Kim, J.S. Lindsey, Tetrahedron 63 (2007) 3826–3839.
- [40] M. Ptaszek, B.E. McDowell, J.S. Lindsey, J. Org. Chem. 71 (2006) 4328–4331.
- [41] M. Ptaszek, J. Bhaumik, H.-J. Kim, M. Taniguchi, J.S. Lindsey, Org. Process Res. Dev. 9 (2005) 651–659.
- [42] M.L. Dean, J.R. Schmink, N.E. Leadbeater, C. Brueckner, Dalton Trans. (2008) 1341–1345.
- [43] M. Taniguchi, M. Ptaszek, B.E. McDowell, J.S. Lindsey, Tetrahedron 63 (2007)

- 3840–3849.
- [44] J. Laakso, G.A. Rosser, C. Szijjártó, A. Beeby, K.E. Borbas, *Inorg. Chem.* 51 (2012) 10366–10374.
- [45] K.E. Borbas, V. Chandrasher, C. Muthiah, H.L. Kee, D. Holten, J.S. Lindsey, *J. Org. Chem.* 73 (2008) 3145–3158.
- [46] A.I. Arkhynchuk, A. Orthaber, D. Kovacs, K.E. Borbas, *Eur. J. Org. Chem.* 2018 (2018) 7051–7056.
- [47] T. Umeyama, T. Takamatsu, N. Tezuka, Y. Matano, Y. Araki, T. Wada, O. Yoshikawa, T. Sagawa, S. Yoshikawa, H. Imahori, *J. Phys. Chem. C* 113 (2009) 10798–10806.
- [48] R. Xiong, A.I. Arkhynchuk, D. Kovacs, A. Orthaber, K. Eszter Borbas, *Chem. Commun.* 52 (2016) 9056–9058.
- [49] Y. Chen, L. Xiong, W. Wang, X. Zhang, H. Yu, *Frontiers of Environmental Science & Engineering* 9 (2015) 897–904.
- [50] M. Taniguchi, O. Mass, P.D. Boyle, Q. Tang, J.R. Diers, D.F. Bocian, D. Holten, J.S. Lindsey, *J. Mol. Struct.* 979 (2010) 27–45.
- [51] J.K. Laha, C. Muthiah, M. Taniguchi, B.E. McDowell, M. Ptaszek, J.S. Lindsey, *J. Org. Chem.* 71 (2006) 4092–4102.
- [52] J. Laakso, G.A. Rosser, C. Szijjarto, A. Beeby, K.E. Borbas, *Inorg. Chem.* 51 (2012) 10366–10374.
- [53] H.L. Kee, C. Kirmaier, Q. Tang, J.R. Diers, C. Muthiah, M. Taniguchi, J.K. Laha, M. Ptaszek, J.S. Lindsey, D.F. Bocian, D. Holten, *Photochem. Photobiol.* 83 (2007) 1125–1143.
- [54] Y. Saga, S. Hojo, Y. Hirai, *Bioorg. Med. Chem.* 18 (2010) 5697–5700.
- [55] Y. Hirai, S. Sasaki, H. Tamiaki, S. Kashimura, Y. Saga, *J. Phys. Chem. B* 115 (2011) 3240–3244.
- [56] Y. Hirai, S. Kashimura, Y. Saga, *Photochem. Photobiol.* 87 (2011) 302–307.
- [57] H. Nagatani, H. Watarai, *Anal. Chem.* 70 (1998) 2860–2865.
- [58] J. Helaja, F.-P. Montforts, I. Kipelainen, P.H. Hynninen, *J. Org. Chem.* 64 (1999) 432–437.
- [59] C. Muthiah, D. Lahaye, M. Taniguchi, M. Ptaszek, J.S. Lindsey, *J. Org. Chem.* 74 (2009) 3237–3247.
- [60] R.B. Woodward, V. Skaric, *J. Am. Chem. Soc.* 83 (1961) 4676–4678.
- [61] M. Taniguchi, M.N. Kim, D. Ra, J.S. Lindsey, *J. Org. Chem.* 70 (2005) 275–285.
- [62] K. Aravindu, H.-J. Kim, M. Taniguchi, P.L. Dilbeck, J.R. Diers, D.F. Bocian, D. Holten, J.S. Lindsey, *Photochem. Photobiol. Sci.* 12 (2013) 2089–2109.
- [63] G.W.T.M.J. Frisch, H.B. Schlegel, G.E. Scuseria, M.A. Robb, J.R. Cheeseman, G. Scalmani, V. Barone, B. Mennucci, G.A. Petersson, H. Nakatsuji, M. Caricato, X. Li, H.P. Hratchian, A.F. Izmaylov, J. Bloino, G. Zheng, J.L. Sonnenberg, M. Hada, M. Ehara, K. Toyota, R. Fukuda, J. Hasegawa, M. Ishida, T. Nakajima, Y. Honda, O. Kitao, H. Nakai, T. Vreven, J.A. Montgomery Jr., J.E. Peralta, F. Ogliaro, M. Bearpark, J.J. Heyd, E. Brothers, K.N. Kudin, V.N. Staroverov, R. Kobayashi, J. Normand, K. Raghavachari, A. Rendell, J.C. Burant, S.S. Iyengar, J. Tomasi, M. Cossi, N. Rega, J.M. Millam, M. Klene, J.E. Knox, J.B. Cross, V. Bakken, C. Adamo, J. Jaramillo, R. Gomperts, R.E. Stratmann, O. Yazyev, A.J. Austin, R. Cammi, C. Pomelli, J.W. Ochterski, R.L. Martin, K. Morokuma, V.G. Zakrzewski, G.A. Voth, P. Salvador, J.J. Dannenberg, S. Dapprich, A.D. Daniels, Ö. Farkas, J.B. Foresman, J.V. Ortiz, J. Cioslowski, D.J. Fox, *Gaussian 09*, Gaussian, Inc, Wallingford CT, 2009, p. 2009.
- [64] G. Schaftenaar, J.H. Noordik, *J. Comput. Aided Mol. Des.* 14 (2000) 123–134.